journal

J. Am. Ceram. Soc., 76 [5] 1281–93 (1993)

Tensile Creep and Creep-Recovery Behavior of a SiC-Fiber–Si_3N_4-Matrix Composite

John W. Holmes,*,† Yong H. Park,† and J. Wayne Jones‡

Ceramic Composites Research Laboratory, Department of Mechanical Engineering and Applied Mechanics and Department of Materials Science and Engineering, The University of Michigan, Ann Arbor, Michigan 48109–2125

The tensile creep and creep-recovery behavior of a unidirectional SiC-fiber/Si_3N_4-matrix composite was investigated at 1200°C in air. A primary objective of the study was to determine how various sustained and cyclic creep loading histories would influence the creep rate, accumulated creep strain, and the amount of strain recovered upon specimen unloading. The key results obtained from the investigation can be summarized as follows: (1) A threshold stress of 60 MPa was identified, below which the creep rate of the composite was exceedingly low ($\sim 10^{-12}$ s^{-1}). (2) Periodic fiber fracture was identified as a fundamental damage mode for sustained tensile creep at stresses of 200 and 250 MPa. (3) Because of transient stress redistribution between the fibers and matrix, the creep life and failure mode at 250 MPa were strongly influenced by the rate at which the initial creep stress was applied. (4) Very dramatic creep-strain recovery occurred during cyclic creep; for cyclic loading between stress limits of 200 and 2 MPa, 80% of the prior creep strain was recovered during 50-h-creep/50-h-unloading cycles and over 90% during 300-s-creep/300-s-unloading cycles. (5) Cyclic loading significantly lowered the duration of primary creep and overall creep-strain accumulation. The implications of the results for microstructural and component design are discussed.

I. Introduction

MONOLITHIC ceramics typically do not possess the elevated temperature toughness required for safety-critical designs. For this reason, a considerable amount of effort has been devoted to the development of ceramics reinforced with continuous fibers.[1–12] Potential applications for fiber-reinforced ceramics include gas turbine components, such as combustors, first-stage vanes, and exhaust flaps.[13] Consideration has also been given to the use of these composites in heat exchangers, rocket nozzles, and along the leading edges of next-generation aircraft.[14,15] The reader is referred to Refs. 15 and 16 for additional information concerning potential applications for fiber-reinforced ceramics, and the current status of research in the areas of processing and elevated-temperature mechanical behavior.

Many of the anticipated applications for fiber-reinforced ceramics will involve creep loading under sustained or cyclic loading histories. Our current knowledge of creep deformation processes in ceramic matrix composites comes mainly from studies performed with whisker-reinforced ceramics[17–27] (a review of creep damage accumulation in whisker-reinforced ceramics is given by Wiederhorn and Hockey[25]). To date, only a limited number of experimental and analytical investigations of creep deformation have been undertaken for continuous-fiber ceramic matrix composites.[28–36] Intrinsic differences in the microstructures of whisker- and fiber-reinforced ceramics give rise to fundamental differences in their creep behavior and mechanisms of creep damage accumulation. For example, the development of matrix cracking in continuous-fiber composites will not necessarily result in creep rupture, since the bridging fibers often have sufficient creep strength to transfer load across the crack faces. In comparison, for whisker-reinforced ceramics, the small physical size and lack of connectivity between whiskers limit their ability to transfer the applied creep load across matrix cracks. Moreover, under cyclic creep loading, the bridging effect of whiskers would be expected to decrease as cyclic interfacial wear and matrix creep relaxes the frictional shear stress that is responsible for load transfer. In fiber-reinforced ceramics, interfacial wear caused by repeated cyclic slip in bridging zones would be less deleterious, since load can still be effectively transferred by portions of the fibers that reside outside the slip zones. Moreover, with fiber-reinforced ceramics, complete load shedding from the matrix to more creep-resistant fibers can occur during tensile or compressive creep (the reverse situation, transfer of load from fibers to a more creep-resistant matrix is also possible). This load transfer, which occurs because of mismatch in the elastic moduli and creep rates of the constituents, influences the operative creep damage mechanism(s) as well as the strain recovery behavior of fiber-reinforced ceramics. For example, if the matrix creeps at a much higher rate than the fibers, the matrix stress will relax during tensile creep, while the average stress in the fibers increases as load is shed by the matrix. This relaxation in matrix stress reduces the likelihood of matrix fracture; however, it is possible for the fiber stress to increase to a level that causes fiber fracture within the composite. In whisker-reinforced composites, complete transfer of the applied creep load to the whiskers would not be possible, since the lack of connectivity between the whiskers allows creep of the matrix in regions between the whiskers. In addition to influencing the manner in which microstructural damage accumulates during creep deformation, the degree of load transfer between the constituents will influence the residual stress state that exists in the fibers and matrix upon unloading. This residual stress state can have a strong influence on creep-strain recovery and the post-creep fracture behavior of continuous fiber-reinforced ceramics.[33–36]

The effects of cyclic loading history on creep-strain accumulation, creep rate, and creep-strain recovery have not been investigated for fiber-reinforced ceramics. The present paper makes a start in this direction by examining the phenomenological aspects of the creep and creep-recovery behavior of a hot-pressed SiC_f/Si_3N_4 composite under sustained and cyclic loading histories.

D. S. Wilkinson—contributing editor

*Member, American Ceramic Society.
†Department of Mechanical Engineering and Applied Mechanics.
‡Department of Materials Science and Engineering.

II. Experimental Procedure

(1) Material, Specimen Geometry, and Load Frame

Hot-pressed composites (processed by Textron Specialty Materials, Lowell, MA), consisting of a Si_3N_4 matrix unidirectionally reinforced with 30 vol% SCS-6 SiC fibers, were used in the creep investigation. The continuous SCS-6 fibers, which are manufactured by chemical vapor deposition of β-SiC onto a 33-μm-diameter carbon core, have a nominal diameter of 143 μm (for information concerning the composition, structure and mechanical properties of SCS-6 fibers, the reader is referred to a series of papers by Dicarlo and co-workers[37–39] and a recent paper by Ning and Pirouz[40]). The composition of the matrix powder was 1.25 wt% MgO, 5.00 wt% Y_2O_3, the balance Stark LC-12 Si_3N_4. Tape casting was used to improve the uniformity of fiber spacing and distribution in the composite. Composite plates were hot-pressed in a nitrogen atmosphere for 2 h, at a temperature of approximately 1700°C and pressure of 30 MPa. After processing, the matrix had a porosity content of approximately 3%. A micrograph showing the typical fiber distribution in the hot-pressed billets is given in Fig. 1. The average distance between fibers was 120 μm, with a standard deviation of 33 μm. Although the fiber spacing was relatively uniform, the fiber distribution alternated between cubic and hexagonal packing.

Edge-loaded specimens (Fig. 2) were machined from the hot-pressed plates, using diamond tooling. The specimens had a gage length of 33 mm and an overall length of approximately 127 mm. Since accurate control over the loading and unloading rate of the specimens was required, as well as accuracy in load-train alignment, all creep experiments were conducted on a servohydraulic load frame (Model 810, MTS Systems Corporation, Minneapolis, MN). Specimen strains were monitored using a water-cooled mechanical extensometer that was fitted with large-grain alumina contact rods. A cylindrical induction-heated SiC furnace was used for specimen heating. Uncooled superalloy grips were used to minimize the axial temperature gradient in the specimens.[41] Specimens were heated at a rate of approximately 50°C/min to the creep temperature of 1200°C. Prior to applying the creep load, specimens were held at 1200°C for 60 min to allow the temperature of the specimen, grips, and extensometer to equilibrate. The grips, furnace, and extensometer were enclosed in an isothermal chamber with a volume of approximately 0.5 m^3. During the experiments, the temperature at the center of the specimen gage section was maintained at 1200° ± 1°C (this represents the deviation from the set point with time). For the grips that were utilized, the axial temperature gradient along the 33-mm specimen gage length was approximately 8°C for a central gage-section temperature of 1200°C. Pt/Pt–10% Rh (Type S) thermocouples were used to monitor the specimen temperature and to provide the feedback signal to the temperature controller. During long-term experiments, drift in the thermocouple output can occur if the thermocouple junction becomes contaminated by elements present within the furnace or in the thermocouple insulation. To minimize the possibility of contamination-related thermocouple drift, a closed-end high-purity Al_2O_3 thermowell was used to protect the thermocouple junction and lead wires. After each experiment, the extent of thermocouple drift was determined by comparison with a known reference. For all experiments, the drift in the thermocouple reading was less than 3°C for creep times up to 400 h. Additional details concerning the specimen, grip, and furnace designs can be found in Ref. 41.

The stress–strain behavior of each specimen was recorded during application and removal of the creep load. This data was investigated for compliance changes that would signify the occurrence of microstructural damage (note that only large-scale damage, sufficient in extent to cause a detectable change in specimen compliance, can be inferred from examination of the stress–strain curves). During specimen loading and unloading, load-cell and extensometer data were gathered at a rate of 50 data points per second; during the creep experiments, data were gathered at a rate of 2 to 5 data points per second (a 16-bit data acquisition board was used to gather load-cell and extensometer data (STI Computers, Sunnyvale, CA, Model No. ACM2-16-8)). These data sampling rates required a significant amount of disk storage space. Therefore, after carefully investigating the data to determine if there were any anomalies, such as strain jumps that would signify the development of microstructural damage, the data files were averaged to make the files more manageable (every 10 to 20 points were averaged; prior to averaging, the loading and unloading segments were stored to allow later calculation of the elastic strains during loading and unloading).

Minor fluctuations in the strain readings were randomly observed during a few of the initial creep experiments. The

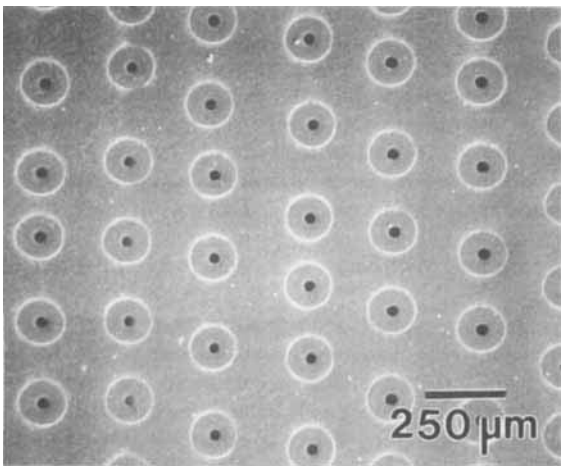

Fig. 1. Fiber distribution in unidirectional SCS-6 SiC_f/Si_3N_4 composites processed by tape casting followed by hot-pressing at 1700°C. The composite contained 30 vol% fibers.

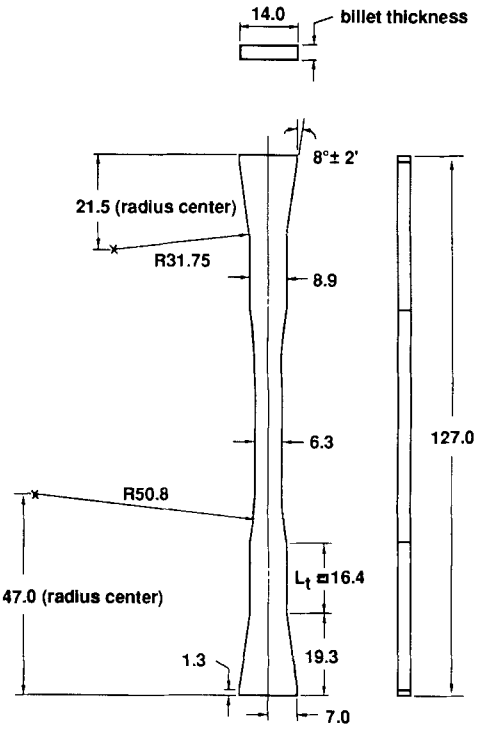

Fig. 2. Edge-loaded tensile specimen used to investigate the creep behavior of SiC_f/Si_3N_4 composites. The specimens are loaded along the tapered (8°) edges. Simpler single-reduction edge-loaded specimens can also be used for the monotonic tension and creep testing of SiC_f/Si_3N_4 composites.[41] Dimensions are given in millimeters.

fluctuations, which had periods ranging from 1 to 20 h, were traced to changes in the temperature and flow rate of the cooling water for the extensometer. Two of the sustained-load creep experiments, conducted under zero load and at 90 MPa, as well as a 400-h cyclic loading experiment, were affected by the fluctuations. Connecting the extensometer cooling water supply to a closed-loop chiller (Cole Parmer Instrument Co., Model No. 12101-10) and flow-rate controller eliminated the fluctuations. Because of the low creep rates encountered, the use of a closed-loop chiller is recommended to anyone contemplating the use of a mechanical water-cooled extensometer for the creep testing of ceramic matrix composites.

(2) Monotonic Tensile Experiments

The monotonic tensile behavior of the composite was determined at 1200°C to provide a comparison with SiC_f/Si_3N_4 specimens used in earlier investigations of creep behavior.[32,33] Previous work[42,43] by the authors had shown that the ambient and elevated temperature monotonic tensile behavior of fiber-reinforced ceramics is strongly influenced by the loading or displacement rate used for testing. At ambient temperature, this loading rate dependence is for the most part caused by slow crack growth. At elevated temperatures, primary creep of the fibers and matrix also contributes to the rate dependence of monotonic tensile behavior. In earlier investigations with SiC_f/Si_3N_4 composites,[32,33] a loading rate of 100 MPa/s was used to minimize time-dependent phenomena; this loading rate was also used in the present investigation.

(3) Sustained Tensile Creep, Creep Recovery, and Postcreep Monotonic Tensile Experiments

The creep behavior of the composite under sustained tensile loading was investigated for applied stresses of 0, 60, 75, 90, 150, 200, and 250 MPa. A virgin specimen was used for each experiment. To obtain a rough indication of the amount of scatter in the data for creep rate and accumulated creep strain, duplicate experiments were conducted for creep stresses of 90 and 200 MPa. As described in the next section, a stress-increment experiment was also conducted to substantiate the experimental trends observed at creep stresses between 60 and 120 MPa. The zero-load experiment was performed to ascertain whether a change in gage-section length, caused by relaxation of processing-related residual stresses or the closure of matrix porosity, would influence the strains measured during the creep- and strain-recovery experiments conducted at higher stresses (for example, a volume contraction caused by additional sintering could lower the apparent creep rate or be confused with creep-strain recovery). The loading and unloading ramps used in the sustained-load and cyclic creep experiments were performed at a rate of 100 MPa/s. For sustained creep loading at 250 MPa, loading rates of 0.25 and 100 MPa/s were compared to determine if relaxation of the matrix stress during initial application of the creep load would influence subsequent creep behavior.

Since the postcreep monotonic tensile behavior of a composite can provide insight into microstructural damage and changes in residual stress state, tensile testing was conducted on specimens that had been crept at stresses of 0, 60, 90, 150, and 200 MPa. Because strain recovery can alter the residual stress state and, therefore, the stress–strain behavior of fiber-reinforced composites,[34-36] the postcreep tensile tests were conducted within 30 s of specimen unloading.

(4) Stress-Increment Experiments

A stress-increment experiment, wherein the creep stress was sequentially increased in small steps, was conducted to provide additional data for the tensile creep rate of the composite between stresses of 60 and 120 MPa. This experiment also provided information regarding the validity of using stress-increment experiments to determine the stress dependence of creep rate for fiber-reinforced ceramics. For the particular loading sequence used, the creep stress was increased in 10-MPa increments from 60 to 80 MPa, followed by 20-MPa increments to 100 and 120 MPa. The creep stress was maintained for 100 h at each stress level and increased at a rate of 100 MPa/s between stress levels (this corresponds to 0.1 or 0.2 s between stresses). For the stresses examined, 100 h was sufficient time for a determination of the quasi-steady-state creep rate to be made.

(5) Cyclic Creep and Creep-Recovery Experiments

The cyclic creep and creep-recovery behavior of the composite was investigated by conducting isothermal experiments at 1200°C with various hold times at a creep stress of 200 MPa and recovery stress of 2 MPa (see Table I); specimens were loaded and unloaded at a rate of 100 MPa/s between these two stresses. To determine the influence of cycle period on accumulated creep strain and creep strain recovery, long-duration 50-h-creep/50-h-recovery cycles were compared with short-duration 300-s-creep/300-s-recovery cycles. To examine how cyclic loading without a recovery hold time would change the overall creep behavior, companion creep experiments were conducted wherein specimens were rapidly unloaded and reloaded at the end of each 50-h or 300-s loading period (2-s unloading and 2-s reloading ramps were used). Schematics of the loading histories and the corresponding idealized strain response of the composite are shown in Figs. 3(A) and (B).

(6) Definition of Creep Rate and Creep-Recovery Strain

Two recovery ratios are defined to quantify the amount of strain recovered after specimen unloading: (1) total-strain recovery ratio and (2) creep-strain recovery ratio. With reference to Fig. 4, the total-strain recovery ratio, R_t, is defined as the sum of the elastic and creep strains recovered in a particular

Table I. Loading Histories Used in the Cyclic-Creep/Creep-Recovery Experiments*

Creep per cycle (s)	Recovery per cycle (s)	Total cycles†	Total test duration (h)
300	0	2384	200
300	300	1192	200
180 000 (50 h)	0	4	200
180 000 (50 h)	180 000 (50 h)	4	400
720 000 (200 h)	90 000 (25 h)	1	125

*In all cases, the creep stress was 200 MPa and the recovery stress was 2 MPa.
†Note that the loading and unloading transients were approximately 2 s each (100 MPa/s).

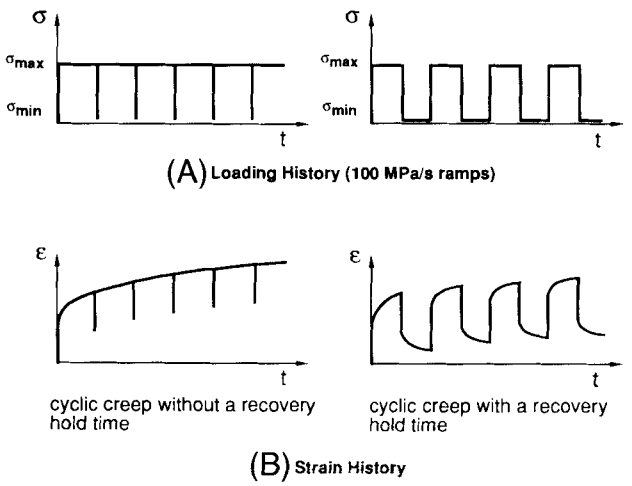

Fig. 3. Cyclic creep experiments. (A) Schematic representation of the cyclic loading histories examined and (B) idealized strain response. For all cyclic creep experiments, the creep stress (σ_{max}) was fixed at 200 MPa and the recovery stress (σ_{min}) at 2 MPa. The loading and unloading ramps were performed at 100 MPa/s.

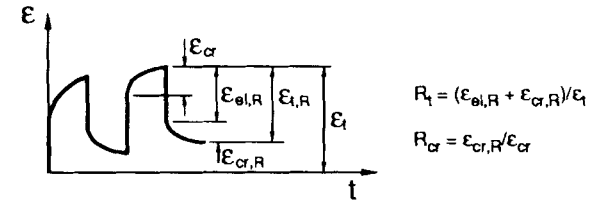

Fig. 4. Definition of the total-strain recovery ratio (R_t) and creep-strain recovery ratio (R_{cr}) used to quantify the amount of strain recovery during the cyclic creep experiments.

cycle ($\varepsilon_{el,R} + \varepsilon_{cr,R}$), divided by the total accumulated strain (including elastic strain) that exists prior to unloading ε_t:

$$R_t = (\varepsilon_{el,R} + \varepsilon_{cr,R})/\varepsilon_t \quad (1)$$

When calculating R_t, the recovered elastic strain is found by examination of the stress–strain data collected during each loading and unloading transient. The creep-strain recovery ratio, R_{cr}, is defined as the creep strain recovered during a particular unloading cycle $\varepsilon_{cr,R}$, divided by the creep strain for the cycle ε_{cr}:

$$R_{cr} = \varepsilon_{cr,R}/\varepsilon_{cr} \quad (2)$$

Note that the instantaneous elastic strain during loading and unloading is not included when calculating R_{cr}.

III. Results and Discussion

(1) Monotonic Tensile Behavior

Figure 5 shows the monotonic tensile behavior of the composite at 1200°C. Under a loading rate of 100 MPa/s, the composite exhibits nearly linear stress–strain behavior to failure, with an ultimate strength of approximately 385 MPa and Young's modulus of 280 ± 10 GPa. From Fig. 5, the creep stresses used in the investigation ranged from approximately 15% to 65% of the ultimate strength. As discussed later, the linear stress–strain behavior does not preclude the occurrence of microcracking during initial loading, nor the absence of matrix or fiber fracture occurring shortly after reaching a particular creep load.

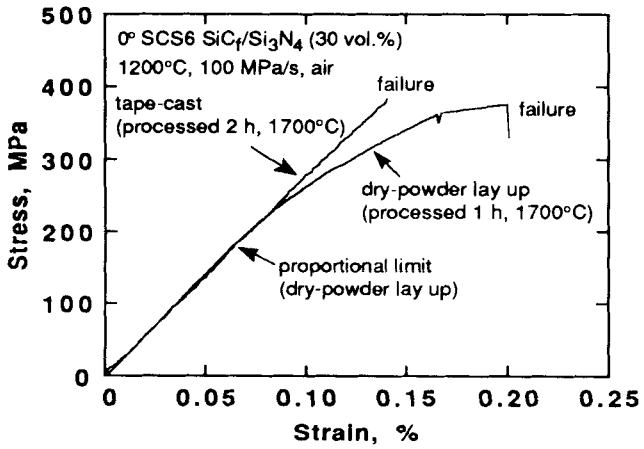

Fig. 5. Typical 1200°C monotonic tensile behavior of the 0° SCS-6 SiC_f/Si_3N_4 composite used in the present investigation (the composite was hot-pressed at 1700°C for 2 h at 30 MPa). For comparison, the monotonic tensile behavior of an earlier 0° SCS-6 SiC_f/Si_3N_4 composite processed by a dry-powder layup approach is shown (hot-pressed at 1700°C for 1 h at 70 MPa).[32] To minimize time-dependent phenomena, the monotonic tension experiments were conducted in air at a constant loading rate of 100 MPa/s.

The brittle stress–strain behavior is attributed to strong interfacial bonding caused by the long hot-pressing time (2 h) used to consolidate the particular billets used in the investigation. Fiber pullout lengths were less than 0.5 mm, indicative of brittle, low-toughness behavior. Earlier work on a similar composite system that was hot-pressed for a shorter time (1 h at 1700°C) showed distinctly nonlinear tensile behavior and significant fiber pullout during tensile testing at 1200°C[32] and 1350°C[33] (for comparison with the present composite, the 1200°C tensile curve is plotted in Fig. 5). The linear tensile behavior found for the tape-cast composite is undesirable from a toughness point of view. However, the creep testing of this composite provided us with a unique opportunity to investigate creep behavior at stress levels that were above the proportional limit stress (≈195 MPa) of SiC_f/Si_3N_4 composites used in previous investigations of creep and fatigue behavior.[32]

(2) Tensile Creep Behavior

In this section, a general overview of the stress dependence of tensile creep behavior is provided. Also discussed is the influence of initial loading rate on the creep life at 250 MPa. The stress dependence of creep rate is discussed in detail in Section III(4). The key figures for this section are Fig. 6, which shows typical sustained-loading creep curves for stresses from 0 to 200 MPa, and Fig. 7 which shows the creep behavior under a stress of 250 MPa. For convenience, the stress dependence of creep behavior and creep-strain accumulation are discussed sequentially, starting with the zero-load experiment.

(A) Zero Load: Isothermal exposure at 1200°C for 200 h under zero load produced no detectable change in specimen gage length (see Fig. 6 for the strain versus time curve), suggesting that processing-related residual stresses were low. Had the initial residual stresses been high, a redistribution in axial stress between the fibers and matrix would be expected to cause a time-dependent change in specimen length during high-temperature exposure. This result also indicates that additional sintering of the matrix or closure of porosity, which would decrease the specimen volume, was insufficient in extent to be detected and, therefore, of no significance to subsequent measurement of creep strains at higher stresses. It is therefore reasonable to assume that the strains measured under the test conditions described in this paper result from creep or creep-recovery processes.

(B) 60 MPa: At 60 MPa, an initial region of transient creep, followed by a near-zero creep rate, was observed. The transient creep extended for approximately 25 h. This creep behavior can be understood by examining the stress state of the

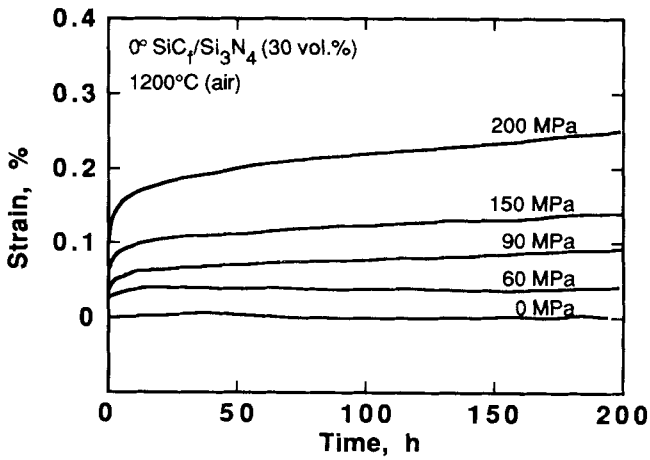

Fig. 6. Typical tensile creep curves for sustained loading of 0° SCS-6 SiC_f/Si_3N_4 at stresses from 0 to 200 MPa. In all cases, specimens were loaded to the creep stress at rate of 100 MPa/s. The creep curves include the instantaneous elastic strain that occurred during specimen loading (at 200 MPa, the elastic strain was approximately 0.07%). At 60 MPa, the creep rate was below 10^{-12} s^{-1}.

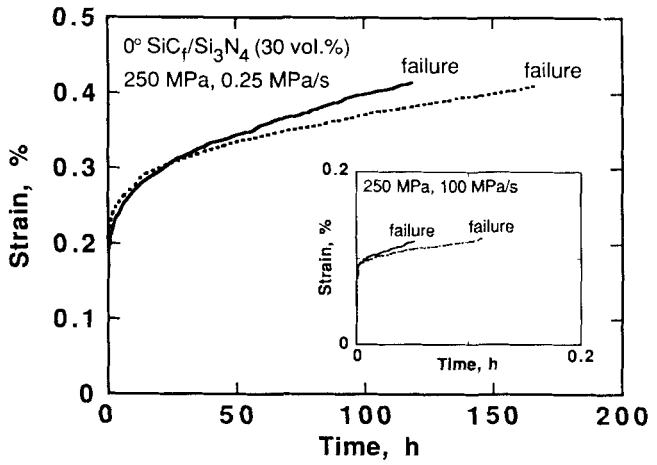

Fig. 7. Tensile creep curves found for sustained loading of 0° SCS-6 SiC_f/Si_3N_4 at 250 MPa. To examine the influence of initial stress relaxation in the matrix on creep life, specimens were loaded to 250 MPa at either 0.25 or 100 MPa/s (see inset). As discussed in the text, loading slowly to the creep stress allows the matrix stress to relax, decreasing the likelihood of matrix fracture and dramatically increasing creep life.

composite that exists immediately after application of the creep load. Upon reaching a creep stress of 60 MPa, the matrix stress would be approximately 55 MPa if calculated by the rule of mixtures (taking E_f = 365 GPa, E_m = 275 GPa, and neglecting processing-related residual sresses). Since this stress is high enough to cause creep of hot-pressed Si_3N_4[45-47] at 1200°C, a redistribution of stress between the fibers and matrix will occur, regardless of whether the fibers also undergo creep. This redistribution in internal stress, where the matrix creeps and sheds load to the more creep-resistant fibers, provides a small region of transient creep. If the temperature and stress are such that the fibers *do not* creep (i.e., undergo only elastic loading), the creep rate of the composite would approach zero once the applied load was completely transferred to the fibers. This sequence of events appears to occur in the SiC_f/Si_3N_4 composite studied here, where, after an initial transient, the creep rate decreased to a level below the resolution of the extensometer ($\approx 10^{-12}$ s^{-1} under ideal conditions). As discussed later, the near-zero creep rate observed at 60 MPa suggests the existence of a threshold stress for the tensile creep of SCS-6 fibers.

(C) 75 to 200 MPa: Creep at stresses between 75 and 200 MPa was characterized by a distinct primary creep regime, followed by a region of relatively constant, but decreasing, creep rate. For purposes of discussion, the region of relatively constant creep rate will be referred to as the *quasi-steady-state* creep regime. Primary creep extended for approximately 50 to 75 h; quasi-steady-state creep continued to the completion of the experiments at 200 h. It is not clear if quasi-steady-state creep would persist during longer-duration creep testing, or if it represents transient behavior that appears to be steady-state because of the limited duration of the creep experiments. As summarized in Table II, the total strain that accumulated in 200 h was low, ranging from 0.06% at 75 MPa to 0.25% at 200 MPa (these strain values include the instantaneous elastic component upon specimen loading, which was approximately 0.021% at 60 MPa and 0.072% at 200 MPa). It is not known at this time if a simple redistribution in stress between the fibers and matrix is the only mechanism responsible for the decelerating creep rate during primary creep. Other mechanisms, such as microstructural evolution in the fibers and matrix, could contribute to the decrease in creep rate. Although not examined in the present study, structural evolution in the fibers, such as an increase in grain size, is expected to be minimal because of the high temperature (1700°C) used for hot-pressing. Identification of the precise mechanisms responsible for the transient creep behavior can be answered only through detailed microstructural examination of specimens that have been interrupted at various stages of the creep process, and through parallel mechanics modeling that determines the extent to which the observed damage would impact strain accumulation and creep rate.

(D) 250 MPa: The creep behavior of the composite at 250 MPa was strongly influenced by the rate at which the creep stress was initially applied. Based upon results obtained from two experiments, loading to the creep stress at a rate of 100 MPa/s resulted in failure in under 400 s (see inset in Fig. 7; as discussed below, creep life improved significantly when the creep stress was applied at a much lower rate). Examination of the stress–strain response of specimens during *initial* loading showed no evidence of a compliance change that would signify the occurrence of large-scale microstructural damage such as matrix or fiber fracture. It is possible, however, that initial microstructural damage which is not sufficient in extent to cause a pronounced compliance change occurs during loading or shortly after reaching the creep stress.

Finite-element analysis of the tensile creep deformation of hot-pressed SiC_f/Si_3N_4 composites has shown that the tensile stress developed in the matrix reaches a maximum at the end of the initial loading transient.[34] After this maximum, the matrix stress rapidly decays as it creeps and sheds load to the more creep-resistant fibers. Thus, the matrix would be most susceptible to fracture at the end of the initial loading transient or during the initial stages of creep. Based upon this premise, it was postulated in the present study that the creep life of the composite would increase if the matrix stresses were permitted to relax during initial loading to the creep stress. Since the matrix sheds load to the fibers, this relaxation could be accomplished by applying the creep stress at a much lower rate. In the limiting case of an infinitesimally slow loading rate, the matrix stress would approach zero if the temperature was sufficiently high to permit matrix creep (this argument assumes that the matrix creeps at a higher rate than the fibers). To experimentally study the effect of initial loading rate on creep life and failure mode, two additional specimens were loaded at a rate of 0.25 MPa/s to the creep stress of 250 MPa (i.e., 1000 s to reach 250 MPa versus 2.5 s for a loading rate of 100 MPa/s). As shown in Fig. 7, the creep life increased dramatically for the slower loading rate, with one specimen surviving 118 h and the other 167 h. These results provide convincing support for a mechanism of creep failure based upon initial matrix fracture. For lower creep stresses, where the initial matrix stress at the end of the loading transient is below the *in situ* fracture strength of the matrix, the creep life should be relatively insensitive to initial loading rate. *To summarize, for high creep stresses, the results indicate a strong loading rate dependence of creep life for brittle matrix composites.*

(3) Microstructural Damage Modes

Periodic fiber rupture was identified by optical and SEM examination as the principal creep damage mechanism that occurred during sustained creep loading at stresses of 200 MPa. By progressive sectioning of the composite, it was estimated that approximately 40% of the fibers had undergone fracture within the gage section. At 250 MPa, periodic fiber rupture was observed only for the specimens that had been loaded to the creep stress at a rate of 0.25 MPa/s; in this case, close to 75% of the fibers had undergone periodic fracture. In contrast, *matrix fracture* appears to have precipitated the failure of specimens that were loaded to 250 MPa at a rate of 100 MPa/s (further details of the microstructural damage that occurred during the creep experiments will be provided in a future paper devoted to creep damage mechanisms in hot-pressed and reaction-bonded Si_3N_4 composites).

Periodic fiber fracture is expected to be a fundamental damage mode for other composite systems where the tensile creep resistance of the fibers exceeds that of the matrix. This damage mode is possible only if simultaneous matrix fracture can be avoided; for example, when weak interfacial bonding is present

Table II. Summary of Loading Histories and Experimental Results*

Loading history	Total cycles	Avg creep rate† (s^{-1})	Total strain (%) (at 200 h)	R_f (%) (first/last cycle)
60 MPa, 200 h	1	$<10^{-12}$	0.04	
75 MPa, 200 h	1	2.8×10^{-10}	0.06	
90 MPa, 200 h	1	3.8×10^{-10}	0.09	
90 MPa, 200 h	1	3.9×10^{-10} (at 100 h)‡	0.07 (at 100 h)	
150 MPa, 200 h	1	5.4×10^{-10}	0.14	
200 MPa, 200 h (+ 25-h recovery)	1	8.6×10^{-10}	0.27	45 (1 cycle)
200 MPa, 200 h (+ 25-h recovery)	1	8.3×10^{-10}	0.26	46 (1 cycle)
250 MPa (100 MPa/s)	1	Failed at ≈210 s	$\varepsilon(200\text{ s}) \approx 0.12$	
250 MPa (100 MPa/s)	1	Failed at ≈402 s	$\varepsilon(400\text{ s}) \approx 0.12$	
250 MPa (0.25 MPa/s)	1	2.9×10^{-9} (failed at 118 h)	$\varepsilon(118\text{ h}) \approx 0.42$	
250 MPa (0.25 MPa/s)	1	1.8×10^{-9} (failed at 167 h)	$\varepsilon(167\text{ h}) \approx 0.41$	
Cyclic 300 s/0 s	2384	7.8×10^{-10}	0.30	≈0/0
Cyclic 300 s/300 s	1192	2.5×10^{-10}	0.13	90/58
Cyclic 300 s/300 s	1192	2.3×10^{-10}	0.12	92/60
Cyclic 180 000 s/0 s	4	8.5×10^{-10}	0.26	≈0/0
Cyclic 180 000 s/180 000 s	4		$\varepsilon(200\text{ h}) = 0.20$ $\varepsilon(400\text{ h}) = 0.26$	61/50

*All cyclic creep experiments were conducted in air at 1200°C between stress limits of 200 and 2 MPa. The creep rates for the stress increment experiment conducted between 60 and 120 MPa are given in Fig. 8. †Average creep rate between 100 and 200 h; at 100 h if failure occurred in under 200 h. ‡Equipment failure at 110 h.

or crack deflection occurs along the fiber/matrix interface (note that the radial stress at the fiber/matrix interface relaxes during long-term creep deformation of SiC_f/Si_3N_4 composites; this would have the effect of decreasing the interfacial shear stress).[34] It is not known at this time if the fiber fractures occurred during transient creep or during the later stages of creep deformation. Thus, a portion of the strain accumulation during transient creep could have been caused by progressive fiber rupture. Studies are currently under way to document how fiber damage evolves during creep deformation.

A question that arises is why the numerous fiber fractures did not cause discontinuous strain jumps in the creep curves. This can be qualitatively answered by noting that the distance over which the matrix supports the load near the ends of a fractured fiber is small (of the order of micrometers, depending upon the load and interfacial shear stress). Since this distance is small, and since the matrix modulus is still high at 1200°C, the instantaneous increase in gage-section displacement is exceedingly small. Strain jumps would be expected only if multiple fiber fractures occurred simultaneously or if matrix fracture accompanies fiber fracture. At 1350°C, where the modulus of the composite is lower, discontinuous strain jumps were observed during the tensile creep of hot-pressed SiC_f/Si_3N_4 composites.[33] An additional question relates to the early failure of the specimens that were rapidly loaded to 250 MPa. For these specimens, failure occurred within 200 to 400 s of reaching the creep stress. Although a compliance change during initial loading was not observed, this does not preclude the initiation of matrix damage during the loading transient. It has been shown by various investigators[48–51] that the onset of matrix fracture during the uniaxial tensile loading of fiber-reinforced composites can occur within the linear portion of a stress–strain curve; however, the resolution of most extensometers is not sufficient to detect the small compliance change that accompanies initial matrix damage. Postcreep examination showed an absence of matrix cracking in the specimens crept at stresses of 200 MPa or lower, indicating that the matrix cracking initiated above 200 MPa. Thus, matrix cracking most likely initiated during initial loading between 200 and 250 MPa, or shortly after reaching the creep stress. Several factors determine if fracture of the bridging fibers occurs after matrix cracking: (1) the residual fiber strength after processing, (2) the inherent creep strength of the fibers, and (3) the degree of interfacial bonding. As a consequence of the high temperature (1700°C) used during hot-pressing, the residual fiber strength will be much lower than that for virgin fibers. For example, Bhatt[52] found that the strength of virgin SCS-6 fibers decreased from an average of 3.8 GPa to less than 0.8 GPa after heat treatment for 1 h at 1850°C. If it is assumed, as a very rough approximation, that a matrix crack extends completely across the specimen, a simple rule-of-mixtures calculation would give an average fiber stress of approximately 830 MPa. Although speculative, the short creep life found for rapid loading to 250 MPa is most likely caused by a combination of matrix crack growth and the fracture of fibers that bridge matrix cracks. Under this scenario, the low residual strength of SCS-6 fibers after exposure to the extremely high temperatures used to consolidate Si_3N_4 will limit the upper creep strength of hot-pressed SiC_f/Si_3N_4 composites (reaction-bonded silicon nitride composites, which are processed at lower temperatures, are expected to have a much higher creep strength).

(4) Stress Dependence of Tensile Creep Rate

The stress dependence of average tensile creep rate between 100 and 200 h is plotted in Fig. 8 for the sustained-load experiments conducted at stresses of 60 to 250 MPa. Also shown in Fig. 8 are the 100-h creep rates obtained from the incremental loading experiment conducted at stresses of 60, 70, 80, 100, and 120 MPa. There was excellent agreement between the results obtained from the continuous-loading and incremental-loading experiments. For comparison, tensile creep rate data obtained from an earlier investigation[32] of SCS-6 SiC_f/Si_3N_4 composites are shown in Fig. 8. The differences in creep rate found between the earlier investigation and the present study are discussed in detail below.

For discussion purposes, the stress dependence of quasi-steady-state creep rate can be divided into three regimes: (1) below 75 MPa, (2) between 75 and 200 MPa and, (3) between 200 and 250 MPa. As noted earlier, the creep rate of the composite at 60 MPa was exceedingly low, suggesting the existence of a threshold stress for tensile creep at 1200°C (see discussion below). Within the range of 75 to 200 MPa, the creep rate exhibited a low stress sensitivity, with a stress exponent, n, of approximately 1 ($\dot{\varepsilon} = B\sigma^n$, where $\dot{\varepsilon}$ is the quasi-steady-state creep rate, B is a constant, and σ is applied stress). The increase in creep rate at 250 MPa was most likely a consequence of the extensive periodic fiber rupture that occurred during creep deformation (this holds only for the slowly loaded specimens; the rapidly loaded specimens failed in under 400 s).

(A) Discussion of Threshold Stress for Tensile Creep: At 60 MPa, the average creep rate between 100 and 200 h was the order of 10^{-12} s^{-1}.§ Assuming, for an upper bound, that the

§The resolution of the extensometer and signal conditioner was such that 10^{-12} s^{-1} was the lowest creep rate that could be measured when averaged over a 100-h period. Thus it could not be unequivocally proved in the present study if creep deformation stops completely at 60 MPa. However, for purposes of discussion, and in a practical sense, the stress at which the creep rate approaches 10^{-12} s^{-1} is defined in this paper as the threshold stress for creep deformation.

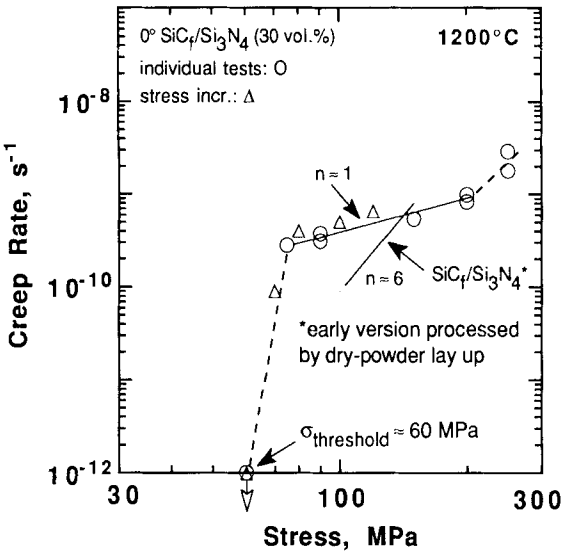

Fig. 8. Quasi-steady-state creep rate versus applied stress for the 1200°C tensile creep of 0° SCS-6 SiC_f/Si_3N_4. The creep rate measured for individual sustained creep loading experiments was similar to that found from a stress-increment experiment conducted at stresses of 60, 70, 80, 100, and 120 MPa. Except for the creep experiments performed at a stress of 250 MPa, all specimens were initially ramped to the creep stress at a rate of 100 MPa/s. A creep threshold, below which the creep rate is exceedingly low, exists at 60 MPa. Results are also shown for an earlier 0° SCS-6 SiC_f/Si_3N_4 composite that was processed by a dry-powder layup technique.[32]

matrix does not contribute to the creep strength of the composite, a simple rule-of-mixtures calculation gives an approximate threshold stress of 200 MPa for the tensile creep of SCS-6 fibers at 1200°C (calculated by dividing the nominal applied stress of 60 MPa by the fiber volume fracture of 0.3). This value serves only as a rough approximation, since the actual stress state of the fibers within the composite is not uniaxial because of mismatch in the elastic constants of the fibers and matrix and the development of hydrostatic stresses between the fibers (hydrostatic stresses develop as a consequence of the constraint to matrix deformation provided by the rigid, closely packed, fibers). Furthermore, it must be appreciated that the threshold stress will depend upon the processing temperature and time, both of which can influence the grain size and, hence, the creep rate of SCS-6 fibers. For example, DiCarlo[37] has shown that prior isothermal exposure of SCS-6 fibers in argon at 1150° to 1360°C increased their creep resistance during subsequent tests conducted between 1200° and 1300°C. Microstructural changes (grain growth) and the removal of free silicon in the fibers were identified by DiCarlo as the mechanisms responsible for the enhanced creep resistance. No information is available in the literature concerning the existence of a threshold stress for creep of SCS-6 fibers. However, a threshold stress for tensile creep deformation has been identified for other SiC fibers; Simon and Bunsell[54] have reported a threshold stress of approximately 150 MPa for the tensile creep of ceramic-grade NPL-102 Nicalon SiC fibers at 1200°C.

(B) Comparison with Previous Tensile Creep Results for Hot-Pressed SiC_f/Si_3N_4: The tensile creep rate of 0° SCS-6 SiC_f/Si_3N_4 composites has been previously studied at 1200°C for stresses from 99 to 135 MPa. Creep rupture data were also obtained at stresses of 150, 175, and 200 MPa.[32] Although the volume fraction of fibers (30 vol%) and matrix composition were nominally the same as that for the tape-cast composite investigated here, the earlier composites were processed at a higher pressure (70 versus 30 MPa) and for a shorter time (1 versus 2 h). There were also minor differences in matrix porosity; the tape-cast composites had a porosity level of approximately 3%, compared to less than 2% for the earlier dry-powder layup composites. The slightly higher porosity content of the tape-cast composite is attributed to the lower pressure used during hot-pressing. The different processing conditions, which would be expected to influence residual stresses and the degree of interfacial bonding, produced significant changes in the monotonic tensile behavior of the two composites (see Fig. 5).[¶] Compared to the tape-cast composite, the dry powder layup composite exhibited a slightly lower creep rate at stresses below approximately 150 MPa (it should be noted that there was approximately an order of magnitude scatter in creep rate for the experiments conducted with the dry-powder layup composites,[32] so the difference in creep rates between the two composites is somewhat subjective). What clearly differed, however, was the creep rupture time for stresses above 150 MPa. In the earlier experiments, creep failures were observed in less than 100 h at 175 MPa and in under 160 h at 200 MPa. In the present study, specimens survived 200 h at 200 MPa. Postcreep SEM examination of specimens crept at 200 MPa and lower showed no evidence of matrix damage. Thus, the improved creep life of the tape-cast composite is attributed, in part, to the avoidance of matrix cracking during initial loading to the creep stress and during subsequent creep deformation. The importance of matrix cracking on creep life can be inferred from the creep experiments conducted at 250 MPa; the creep life increased considerably when initial matrix fracture was delayed by slowly loading to the creep stress. Although the improved creep life of the tape-cast composite may be desirable for certain applications, there is an important tradeoff; namely, the tape-cast composite had a significantly lower toughness (as shown by the brittle stress–strain behavior observed in virgin specimens and after creep deformation—see later discussion of postcreep monotonic tensile behavior).

In the earlier study[32] with SiC_f/Si_3N_4 composites, a stress exponent of 6 was found for the stress dependence of quasi-steady-state creep rate between stresses of 99 and 135 MPa. This compares with a stress exponent of approximately 1 found in the present study for stresses between 75 and 200 MPa. The different stress exponents suggest different creep damage mechanisms. The earlier composites also contained numerous regions where the matrix oxides (MgO and Y_2O_3) used to promote sintering during hot-pressing were not completely dispersed. In addition to promoting fiber degradation,[33] the presence of these oxide-rich regions would change the microcracking characteristics of the matrix during initial loading and subsequent creep deformation; although speculative, this offers a plausible explanation for the low creep-rupture life found for stresses above 150 MPa. It is also possible that the creep characteristics of the earlier composites were influenced by the higher processing pressure, which could potentially impact both the residual stress state and interfacial bonding present in the composite and, hence, the manner in which microstructural damage accumulates during creep.

(5) Cyclic Creep and Strain Recovery

Figures 9(A)–(D) compare the cyclic creep behavior of specimens subjected to the following loading histories: (1) 50-h creep/50-h recovery, (2) 50-h creep/0-s recovery, (3) 300-s creep/300-s recovery, and, (4) 300-s creep/0-s recovery. The total test duration and number of loading/unloading cycles for each loading history are summarized in Table I.

(A) Influence of Cyclic Loading on Initial Transient (Primary) Creep Behavior: For the 50-h-creep/50-h-recovery cycles, transient (primary) creep, characterized by rapid strain accumulation, but a decreasing creep rate, persisted for the first 50 h of creep (see Fig. 9(A)). During subsequent cycles, the duration of transient creep decreased to approximately 25 h per cycle. The introduction of a rapid unloading and reloading

[¶] Recent optimization of processing parameters has provided tape-cast SiC_f/Si_3N_4 composites with much higher failure strains (at 1200°C and a loading rate of 100 MPa/s these composites exhibit a distinct proportional limit stress between 100 and 250 MPa with failure strains approaching 0.3 to 0.4%).[53]

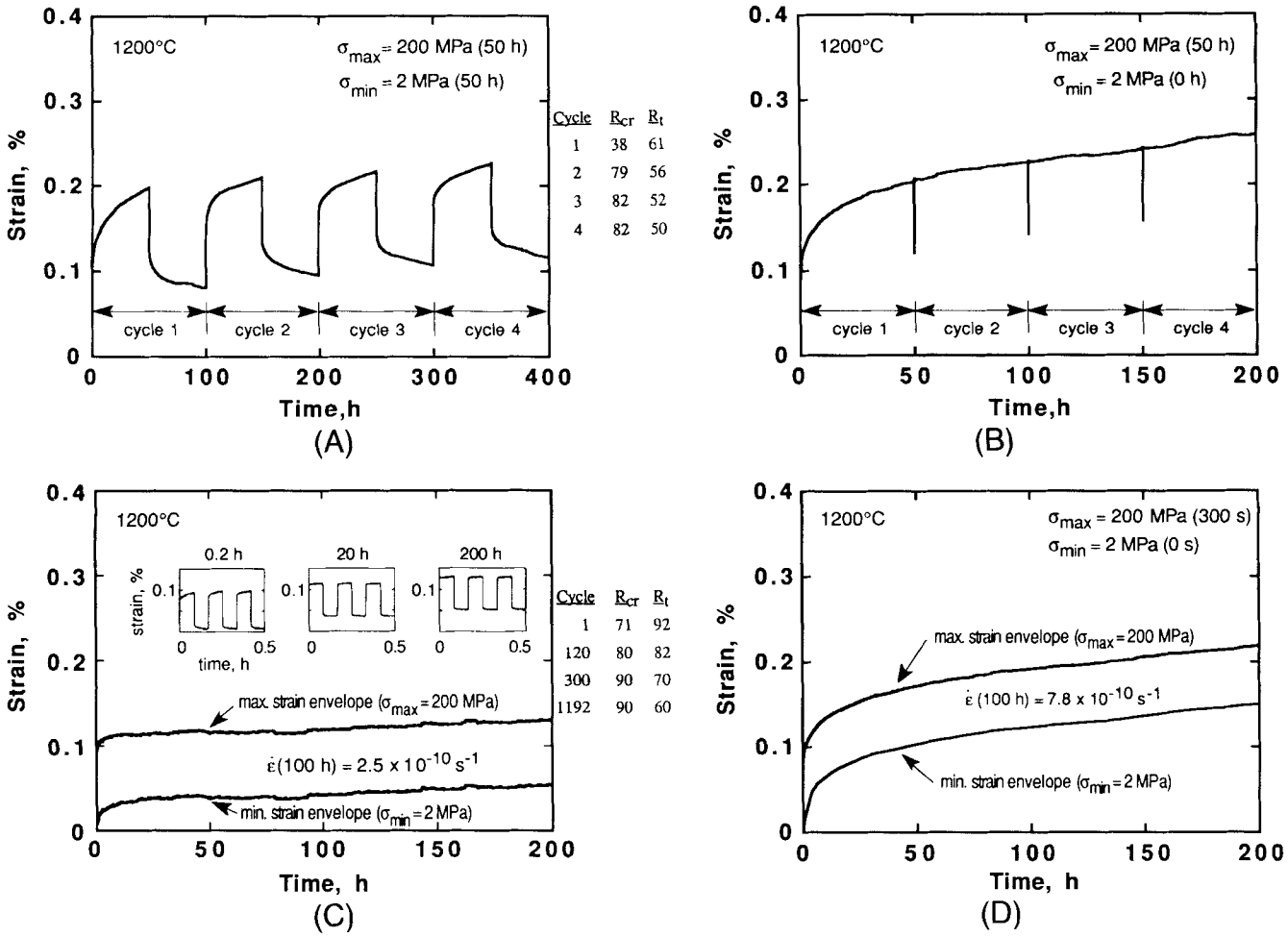

Fig. 9. Isothermal (1200°C) cyclic creep behavior of 0° SCS-6 SiC_f/ Si_3N_4. Specimens were cycled between stress limits of 200 and 2 MPa. For loading histories with a finite recovery hold time, the total-strain recovery and creep-strain recovery ratios ($R_t = (\varepsilon_{el,R} + \varepsilon_{cr,R})/\varepsilon_t$ and $R_{cr} = \varepsilon_{cr,r}/\varepsilon_{cr}$, respectively) are shown adjacent to the creep curves. (A) 50-h creep/50-h recovery. (B) 50-h creep/0-s recovery. (C) 300-s creep/300-s recovery. (D) 300-s creep/0-s recovery.

cycle every 50 h, without a recovery hold period, did not introduce transient creep on reloading, the prior creep rate was immediately reestablished (see Fig. 9(B)). A significant change in primary creep behavior was found for the shorter-duration 300-s-creep/300-s-recovery cycles (Fig. 9(C)). For this loading history, the duration of transient creep was reduced to less than 20 h, versus roughly 70 h for sustained creep at 200 MPa. The insets in Fig. 9(C) show the creep behavior of the composite at selected times. Beyond approximately 20 h, the strain versus time curves showed very little hint of transient creep upon reloading. As discussed below, the accumulated creep strain was significantly less than that for sustained creep loading at 200 MPa. Compared to sustained creep at 200 MPa, no significant change in overall tensile creep rate was found when the recovery period was eliminated by rapid unloading and reloading every 300 s; there was, however, a reduction in total accumulated creep strain. The reduction in accumulated strain appears to be caused by strain recovery that occurs during the 2-s unloading and 2-s reloading ramps (specimens were unloaded and reloaded at a rate of 100 MPa/s—for the 300-s-creep/0-s-recovery loading history this amounts to roughly 8000 s at stress levels below 200 MPa).

(B) Creep Strain Accumulation and Creep Rate: Figures 10 and 11 compare the strain–time behavior for cyclic and sustained creep loading at 200 MPa. To reflect the shorter time spent at maximum load during the cyclic creep experiments, the cyclic creep data have been "compressed" by removing the unloading periods and plotting only the data for the portions of each cycle that were at a stress of 200 MPa. This procedure allows a comparison of accumulated creep strain to be made for an equivalent amount of time under maximum load. The cycle period has a pronounced effect on creep behavior. For the 50-h-creep/50-h-recovery cycles, only a moderate reduction in accumulated creep strain was observed (Fig. 10). For an equivalent time at 200 MPa, the higher-frequency 300-s-creep/300-s-recovery cycles led to substantial reductions in accumulated creep strain and strain rate (e.g., at 100 h the accumulated strain is 60% lower and the creep rate 43% lower than that found for sustained loading at 200 MPa, see Fig. 11). The reduction in accumulated creep strain found for short-duration cyclic loading is a consequence of the reduced duration of transient creep and the reduction in overall creep rate; as discussed in the next section, strain recovery and accompanying changes in the residual stress state of the composite are responsible for these reductions.

(C) Strain Recovery: Significant strain recovery was observed for the loading histories with a finite recovery hold time. For single-cycle 200-h-creep/25-h-recovery experiments (see Fig. 12), the creep-strain recovery ratio (R_{cr}) was roughly 50% after 25 h of recovery; the total-strain recovery ratio was approximately 45% to 46%. Far more dramatic creep-strain recovery occurred during the multiple-cycle creep experiments that were discussed above. For the four-cycle 50-h-creep/50-h-recovery experiment (Fig. 9(A)), the creep-strain recovery ratio (R_{cr}) increased from approximately 38% for the first cycle to 82% on subsequent cycles. For the higher frequency 300-s-creep/300-s-recovery experiment, R_{cr} increased from approximately 70% during the first few hours of cyclic loading, to 80%

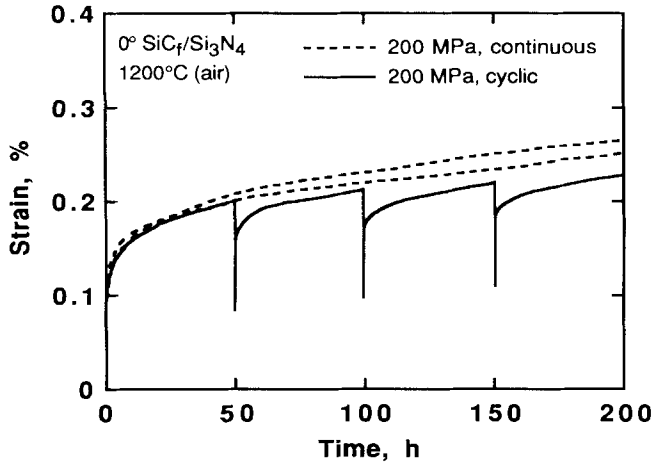

Fig. 10. Comparison of the accumulated creep strain and tensile creep rate for sustained loading at 200 MPa and long-duration cyclic loading (50-h creep/50-h recovery) between stress limits of 200 and 2 MPa. Only the loading portions of the cyclic creep curve are shown (the recovery segments were deleted, and the resulting curves were shifted to the left to allow a comparison of creep strain accumulation to be made for an equivalent time at the creep stress of 200 MPa).

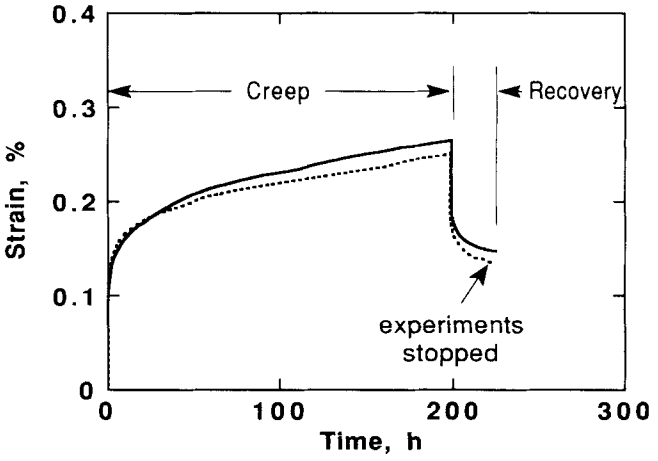

Fig. 12. Creep-recovery behavior of specimens subjected to sustained tensile creep for 200 h at 200 MPa, followed by 25 h of recovery at 2 MPa. After 25 h of recovery, the total-strain recovery ratio ($R_t = (\varepsilon_{el,R} + \varepsilon_{cr,R})/\varepsilon_t$) was approximately 50%.

at 20 h, and 90% at 50 h; thereafter, R_{cr} remained constant for the duration of the 200-h experiment. Strain recovery provides a powerful mechanism for the reduction of creep strain during cyclic creep or fatigue loading. In the absence of cyclic crack growth, the strain recovery is expected to significantly increase the life of cyclically loaded structures.

(D) Microstructural Damage during Cyclic Loading: For cyclic loading without a recovery hold time, the percentage of fiber fractures was similar to that found for sustained loading at 200 MPa. When a 300-s or 50-h recovery hold time was included, the number of fiber fractures decreased (less than 10% of the fibers were fractured for the specimen subjected to 300-s-creep/300-s-recovery cycles, and roughly 30% for the 50-h-creep/50-s-recovery cycles; this compares with approximately 40% fractured fibers for sustained loading at 200 MPa). The decreased number of fractured fibers observed with cyclic loading is attributed to the reduction in fiber stress that occurs during the recovery periods. This brings up an important point:

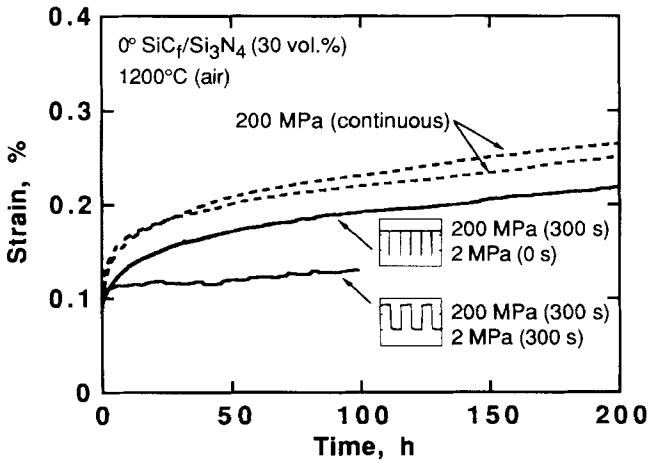

Fig. 11. Comparison of the accumulated creep strain and creep rate for sustained loading at 200 MPa and for short-duration cyclic loading (300-s creep/300-s recovery and 300-s creep/0-s recovery). For the cyclic creep experiments, only the traces of the strain versus time curves obtained at the creep stress of 200 MPa are shown. As in Fig. 10, the recovery segments of each cycle have been removed to allow a comparison of accumulated creep strain to be made for an equivalent time at the creep stress of 200 MPa.

when strain recovery occurs, the rate of microstructural damage and creep-strain accumulation may actually *decrease* under cyclic loading.

(6) Discussion of Mechanical Driving Force for Strain Recovery in Fiber-Reinforced Ceramics

The recovery ratios found for cyclic creep loading are larger than those reported for monolithic Si_3N_4. For example, Arons and Tien[55] observed less than 10% recovery in creep strain for tensile creep experiments conducted with NC-132 Si_3N_4 at 1204°C. Depending upon the amount of prestrain, Haig *et al.*[56] observed up to 40% strain recovery after tensile creep of a fine-grained hot-pressed Si_3N_4 at 1150°C. Strain recovery in monolithic Si_3N_4 is generally attributed to the presence of a glassy grain-boundary phase.[57] In addition to intrinsic strain recovery of the matrix (in particular for Si_3N_4-based composites), two additional mechanisms assist the strain recovery process in fiber-reinforced ceramics: (1) intrinsic recovery of the fibers upon a stress decrement (see Dicarlo[37] for a discussion of anelastic recovery in SCS-6 fibers) and (2) a mechanical driving force that arises from the residual stress state that develops in the composite upon unloading. This residual stress state develops as a result of unequal creep rates and elastic constant mismatch between the fibers and matrix. For the SiC_f/Si_3N_4 composite examined, elastic unloading of the composite after tensile creep places the matrix in compression and the fibers in tension. *In situ* creep of the residually stressed fibers and matrix will relieve the residual stresses if the temperature after unloading is maintained high enough to permit time-dependent creep of at least one of the constituents.

Insight into the changes in fiber and matrix stress that occur during tensile creep and creep recovery can be obtained from Fig. 13, which shows results obtained from an earlier finite-element analysis of creep deformation in unidirectional SiC_f/Si_3N_4 composites.[34] The analysis assumed that at 1200°C the fibers creep at a much lower rate than the matrix. Two limiting cases are shown: (1) perfect interfacial bonding and (2) complete interfacial debonding. The actual interfacial condition would be somewhere between these two ideal cases. For discussion purposes it does not matter which interfacial condition is assumed, since only the initial transient creep behavior is affected.[34] From Fig. 13, the matrix stress reaches its maximum at the end of the initial loading transient, after which the matrix stress relaxes as load is shed to the fibers. Upon unloading from a stress of 200 MPa, elastic contraction of the fibers places the matrix in a state of residual compression. It is important to note that the magnitude of this residual compressive stress is larger than that which existed prior to initial creep loading. To balance the higher

compressive stress in the matrix, the tensile stress in the fibers will be greater than that which existed at the beginning of the creep cycle. During the recovery hold time, the stresses in the fibers and matrix relax (the matrix stress becomes less compressive and the fiber stress less tensile). The extent of stress redistribution that occurs during recovery is influenced by the recovery stress and hold time. Upon reloading, a finite amount of time is required to achieve the prerecovery stress level in the fibers.

Since the stress state of the constituents affects their fracture behavior and intrinsic creep rates (in particular, transient creep rates), the recovery time can have an important effect on the mode of creep damage and overall creep strain accumulation. If a specimen was instantaneously unloaded and reloaded, only elastic deformation would occur and the fiber stress would immediately recover its prior level (in this limiting case, the previous tensile creep rate of the composite would be immediately reestablished). In contrast, if a finite recovery hold time is permitted, the fiber stress will rapidly decrease. During sustained creep loading, the fiber stress will continue to increase until all load is transferred from the matrix. In contrast, for cyclic loading, the fiber stress relaxes during each recovery hold period; upon reloading, the fiber stress is lower than it was at the end of the previous creep period; in other words, the buildup of stress in the fibers occurs at a slower rate than it does under sustained tensile creep loading. Because the mechanical driving force for recovery diminishes as the fiber and matrix stresses relax, the rate of strain recovery decreases rapidly with time. Since the rate of recovery decays in an approximately exponential manner, the majority of recovery takes place shortly after unloading. Thus, compared to fewer cycles of longer duration, numerous short recovery cycles have a far greater impact on reducing the overall rate of strain accumulation.

(7) Postcreep Monotonic Tensile Behavior

Selected specimens were loaded to failure under monotonic tension to ascertain if the various creep experiments had changed the tensile behavior. The tensile experiments were conducted in air at 1200°C. Figure 14 compares the typical monotonic tensile behavior of a virgin specimen with that found for specimens that were subjected to continuous creep at 0, 60, 90, 150, and 200 MPa. For most of the creep-loading histories there was a slight reduction in ultimate strength (between 10% and 35%). In general, the residual strength decreased as the prior creep stress was increased. The exception to this trend was the zero-load creep experiment, which showed the lowest residual strength. The reason for this deviation is not known at this time, however, since only one specimen was tested at zero load; this result may simply represent statistical scatter in the strength. In general, a slight reduction (typically <5%) in modulus was found after sustained and cyclic creep loading.

The reduction in ultimate strength after tensile creep deformation can be explained with reference to Fig. 13, which shows the predicted changes in residual stress state that occur during tensile creep and strain recovery of a SiC_f/Si_3N_4 composite. Immediately after specimen unloading, the residual tensile stress in the fibers will be higher than the tensile stress that existed at the start of the creep experiment. Since the tensile stress in the fibers controls the ultimate strength of the composite, the composite will fracture at a lower applied load. It is important to note that the fiber stress will relax if held at temperature after unloading; thus, the tensile behavior will be influenced by the amount of time that a specimen is held at temperature prior to tensile testing.

As shown in Fig. 15, the composite exhibited minimal fiber pullout during postcreep monotonic tensile testing. The average fiber pullout length increased only slightly after creep loading (typically of the order of 1 mm compared to less than 0.5 mm found after the monotonic tension testing of virgin specimens at 1200°C). This minimal fiber pullout is consistent with the linear stress–strain curves obtained for virgin and crept specimens.

(8) Implications of Results for Cyclic Creep Testing and Determination of Postcreep Residual Strength

As noted earlier, the strain recovery that occurs in fiber-reinforced ceramics imparts a strong loading history dependence to cyclic creep behavior. With regard to creep testing there are several practical consequences of strain recovery:

(1) Careful attention must be given to the rate of loading and unloading used during cyclic creep experiments. Figure 11 shows that even rapid 2-s-loading/2-s-unloading ramps (100 MPa/s) can influence primary creep behavior and total strain accumulation during cyclic creep with a 300-s hold at 200 MPa. It is therefore important to specify the precise loading transients and hold times used in cyclic creep experiments.

(2) Because strain recovery and relaxation of residual stresses occur upon specimen unloading, the postcreep residual strength of a composite will be influenced by the amount of time that a specimen is held at elevated temperature prior to tensile testing. Thus, in addition to specifying the prior loading

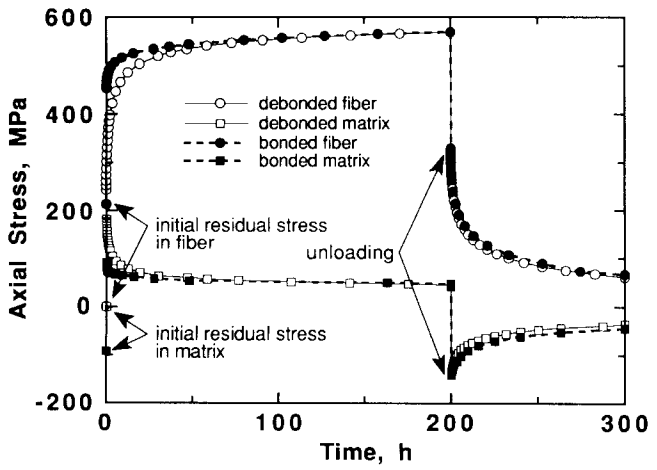

Fig. 13. Changes in fiber and matrix axial stress during creep and creep recovery of SCS-6 SiC_f/Si_3N_4 (results obtained from a 2-D finite-element analysis).[34] The loading history assumed tensile creep at 200 MPa for 200 h, followed by recovery at 2 MPa for 100 h. The residual stress state that exists after specimen unloading provides a mechanical driving force for strain recovery. This mechanical driving force acts in parallel with the intrinsic creep recovery processes that occur in hot-pressed Si_3N_4[55,56] and SCS-6 SiC fibers.[37] As recovery progresses, the driving force for further recovery rapidly diminishes.

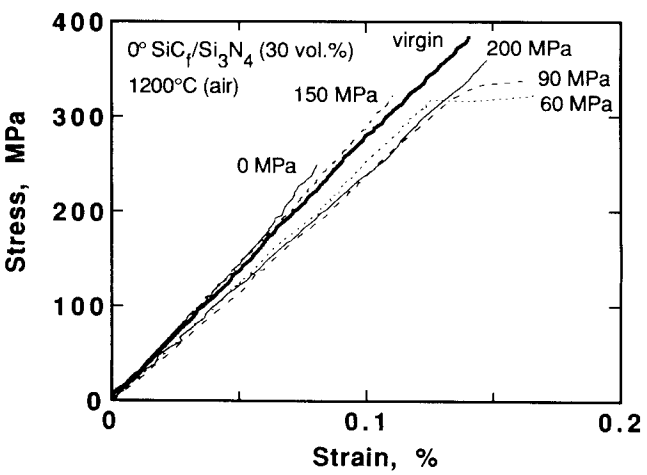

Fig. 14. 1200°C monotonic tensile behavior of 0° SCS-6 SiC_f/Si_3N_4 specimens crept for 200 h at 1200°C. All tension tests were performed within 30 s of removal of the creep stress. In all cases, the specimen strength decreased after creep exposure.

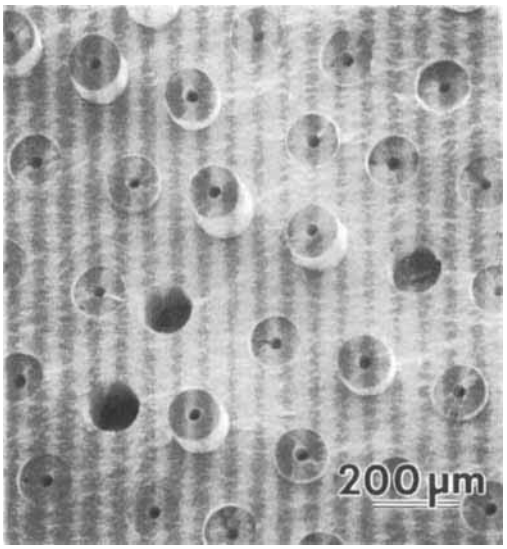

Fig. 15. SEM micrograph showing fiber pullout observed after post-creep monotonic tensile testing of a specimen that had been subjected to 200 h of cyclic creep between stress limits of 200 and 2 MPa.

history of a specimen, it is recommended that the precise thermal history of the specimen be included when reporting residual strength measurements.

(9) Implications of Results for Life Prediction and Engineering Design

The total strain that accumulates during cyclic loading is an important design parameter for many components. It is apparent that under certain cyclic loading conditions, such as cyclic loading with a short duration tensile hold and finite recovery time, component lifetime, based upon total accumulated strain, will actually be extended when compared to sustained creep loading. This increase in life is contrary to what is typically expected for cyclically loaded structures and points to the need to further study the influence of cyclic loading on the creep behavior of continuous-fiber composites.

It may be possible to use knowledge of the creep-strain recovery behavior of composites to increase the service life of future components manufactured from fiber-reinforced ceramics. For example, components that are subjected to tensile creep could be periodically removed from service and isothermally exposed in a furnace under zero load to allow a relaxation of the residual tensile stress in the fibers by strain recovery. This approach would provide a straightforward means by which the life of turbine components and heat exchangers could be extended.

Finally, although the proportional limit stress has been shown to provide a rough predictor of fatigue life for fiber-reinforced SiC_f/Si_3N_4 composites,[32] no such correlation for creep life was observed in this or earlier[33] creep studies. For example, for the particular SiC_f/Si_3N_4 composite used in this investigation, which had no distinct proportional limit, creep failures were observed entirely within the linear region of the initial monotonic tensile curve.

(10) Implications of Results for Microstructural Design

The design of composite microstructures for improved creep resistance is a topic that has received very little attention but is crucial to the use of brittle-matrix materials in applications where creep loading will be encountered. In the present section, the effect of increasing fiber volume fraction or increasing matrix creep resistance on the overall creep behavior of fiber-reinforced composites is discussed. Since fiber creep controls the long-term creep behavior of the hot-pressed SiC_f/Si_3N_4 composites that were investigated, an increase in fiber fraction would decrease the creep rate and total strain accumulation. With an increase in fiber fraction, the average fiber stress decreases and the applied (far-field) stress required to initiate matrix cracking increases. An increase in the matrix cracking threshold would reduce the likelihood that matrix fracture would occur during initial creep loading. It is also important to recognize that the threshold stress for tensile creep, and the amount of strain recovery during cyclic loading, would also be increased by a larger volume fraction of fibers. With regards to the threshold stress for creep, one could tailor the volume fraction of fibers to provide a creep threshold for creep deformation that is above the design stress of a component; designing to a threshold stress would greatly simplify component design.

At low stresses, advanced monolithic silicon nitrides, processed by hot-pressing[47] or reaction bonding,[58] have been shown to have a lower creep rate than the hot-pressed SiC_f/Si_3N_4 composites studied here. Thus, at first glance, it would appear that the creep resistance of SiC_f/Si_3N_4 composites could be improved by using more creep-resistant matrix formulations. However, many of the matrix formulations that provide good creep resistance in monolithic form are not amenable to consolidation when used to manufacture SiC_f/Si_3N_4 composites by hot-pressing. Moreover, other issues must also be examined. For example, if the matrix creeps at a lower rate than the fibers, matrix fracture could occur as load is shed from the fibers to the matrix. For tensile creep loading, this leads to the interesting conclusion that, to reduce the buildup of matrix stress and accompanying matrix-initiated creep failure, it may be desirable to use a matrix that creeps at a higher rate than the fibers.

From the above discussion, it is apparent that increasing the volume fraction of fibers would be the preferred approach for reducing creep rate and strain accumulation in fiber-reinforced ceramics. However, it is important to note that microstructural changes that improve creep resistance, such as increasing the matrix cracking threshold or increasing interfacial shear stress, can have deleterious effects on composite toughness. A delicate balancing act involving changes in the various microstructural parameters will be required to design a composite for applications requiring a combination of high toughness and creep resistance.

IV. Conclusions

The tensile creep and creep recovery behavior of a hot-pressed 0° SCS-6 SiC_f/Si_3N_4 composite was investigated at 1200°C in air. The following conclusions can be made regarding the tensile creep and creep-recovery behavior of the composite:

(1) Periodic fiber fracture was identified as a fundamental damage mode that occurs during long-duration tensile creep loading. Load transfer from the matrix to the more creep-resistant SCS-6 fibers causes the fiber stress to progressively increase during creep, leading to fiber fracture. This damage mechanism would be expected to occur in other fiber-reinforced ceramics where the creep rate of the matrix exceeds that of the fibers.

(2) A threshold stress was identified for tensile creep deformation at 1200°C. At a stress of 60 MPa, the creep rate approached zero within 50 h. The near-zero creep rate is attributed to an apparent threshold stress for creep deformation of SCS-6 SiC fibers at 1200°C. Assuming, as a limiting case, that the matrix does not contribute appreciably to the creep strength of the composite would give an approximate threshold stress for fiber creep of 200 MPa. It was proposed that the threshold stress for creep could be used as a design parameter, and that the threshold stress for composite creep could be increased by increasing the volume fraction of fibers.

(3) Within the range of 75 to 200 MPa, the creep rate of the composite exhibited a low stress sensitivity. When fit to a power-law relationship between creep rate and applied stress ($\dot{\varepsilon} = B\sigma^n$, where $\dot{\varepsilon}$ is the creep rate, B is a constant, and σ is the applied stress), the stress exponent, n, was approximately 1.0.

(4) The tensile creep life of the composite at 250 MPa was strongly influenced by initial loading history. When specimens were loaded to the creep stress in 2.5 s (100 MPa/s), failure was observed in under 400 s. In sharp contrast, loading to the creep stress in 1000 s (0.25 MPa/s) gave creep rupture lives of 120 h or greater. The increase in creep life is attributed to relaxation of the matrix stress that occurs during slow loading. This relaxation reduces the likelihood of matrix fracture during loading and during the initial stage of transient creep.

(5) The creep rate obtained from stress-increment experiments was similar to that found from individual sustained-load creep experiments. These results indicate that rising-load stress-increment experiments, commonly used to characterize the creep behavior of metals and monolithic ceramics, are a viable approach for determining the creep rate of ceramic matrix composites. As a consequence of creep strain recovery during specimen unloading, stress-decrement or strain-decrement experiments would not be suitable for determining the stress dependence of creep rate.

(6) Dramatic strain recovery was observed during cyclic creep loading. The amount of strain recovery was influenced by cycle duration. For example, creep-strain recovery ratios approaching 80% were observed during long-duration (50-h-creep/50-h-recovery) creep cycles between stress limits of 200 and 2 MPa. For the same stress limits, the creep-strain recovery ratio increased to 90% for shorter-duration (300-s-creep/300-s-recovery) creep cycles. In fiber-reinforced composites, the recovery process is assisted by the residual stress state that develops in the composite upon specimen unloading.

(7) The extent of primary creep was significantly reduced for cyclic loading with a finite recovery hold time. Under sustained creep loading at 200 MPa, primary creep persisted for approximately 70 h. For cyclic loading with a 300-s hold at 200 MPa, followed by rapid unloading and reloading (without a recovery hold time), the duration of primary creep was again roughly 70 h. These results compare with less than 20 h of primary creep observed for a cyclic loading with a 300-s hold at 200 MPa followed by 300 s of recovery per cycle.

(8) Strain recovery led to significant reductions in total accumulated creep strain and overall creep rate. For a maximum cyclic stress of 200 MPa, the lowest overall strain accumulation and creep rate occurred when specimens were subjected to short-duration cyclic loading (300-s creep/300-s recovery). A change in the primary creep behavior of the composite was largely responsible for the reduction in accumulated creep strain during cyclic loading. Reductions in the duration of primary creep and overall creep rate are attributed to changes in the residual stress state of the fibers and matrix that occur during the unloading portion of the creep cycle (in the absence of a recovery hold time, the primary creep behavior and creep rate of the composite were essentially unchanged).

(9) It was proposed that knowledge of the creep strain recovery behavior of composites could be used to increase the lifetime of components subjected to sustained or cyclic creep loading. Tensile creep deformation in a composite leads to the development of significant residual tensile stresses in the constituent that has lower creep rate. Periodic removal of a crept component from service, followed by isothermal heating under zero load, would decrease the residual stress and accumulated creep strain.

Acknowledgments: The authors would like to acknowledge funding provided by The University of Michigan, Department of Mechanical Engineering and Applied Mechanics, for the purchase of equipment and to NASA Lewis Research Center which provided both student and equipment support to conduct the research. Appreciation is also expressed to Textron Specialty Materials for processing the composites used in this investigation.

References

[1]K. M. Prewo and J. J. Brennan, "High Strength Silicon Carbide Fiber Reinforced Glass Matrix Composites," *J. Mater. Sci.*, **15,** 463 (1980).

[2]J. J. Brennan and K. M. Prewo, "Silicon Carbide Reinforced Glass Ceramic Matrix Composites Exhibiting High Strength and Toughness," *J. Mater. Sci.*, **17,** 2371–83 (1982).

[3]R. T. Bhatt, "Mechanical Properties of SiC-Fiber-Reinforced Reaction-Bonded Silicon Nitride Composites," NASA Technical Report 85-C-14, 1985.

[4]P. Lamicq, G. A. Bernhart, M. M. Danchier, and J. G. Mace, "SiC/SiC Composite Ceramics," *Am. Ceram. Soc. Bull.*, **65** [2] 336–38 (1986).

[5]M. S. Newkirk, A. W. Urguhart, H. R. Zwicker, and E. Breval, "Formation of Lanxide™ Ceramic Composite Materials," *J. Mater. Res.*, **1** [1] 81–89 (1986).

[6]C. A. Andersson, P. Barron-Antolin, A. S. Fareed, and G. H. Schiroky, "Properties of Fiber-Reinforced LANXIDE™ Alumina Matrix Composites"; pp. 209–15 in Proceedings of the International Conference on Whisker- and Fiber-Toughened Ceramics. ASM International, Materials Park, OH, 1988.

[7]K. M. Prewo, "Fiber-Reinforced Ceramics: New Opportunities for Composite Materials," *J. Am. Ceram. Soc. Bull.*, **68** [2] 395–400 (1989).

[8]W. Foulds, J-F. LeCostaouec, C. Landri, S. DiPierto, and T. Vasilos, "Tough Silicon Nitride Matrix Composites Using Textron Silicon Carbide Monofilaments," *Ceram. Eng. Sci. Proc.*, **10** [9–10] 1083–1099 (1989).

[9]H. Kodama, H. Sakamoto, and T. Miyoshi, "Silicon Carbide Monofilament-Reinforced Silicon Nitride or Silicon Carbide Matrix Composites," *J. Am. Ceram. Soc.*, **72** [4] 551–58 (1989).

[10]T. Yamamura, T. Ishikawa, M. Sato, M. Shibuya, H. Ohtsubo, T. Nagasawa, and K. Okamura, "Characteristics of a Ceramic Matrix Composite Using a Continuous Si-Ti-C-O Fiber," *Ceram. Eng. Sci. Proc.*, **11** [9–10] 1648–60 (1990).

[11]J. R. Strife, J. J. Brennan, and K. M. Prewo, "Status of Continuous Fiber-Reinforced Ceramic Matrix Composite Processing Technology," *Ceram. Eng. Sci. Proc.*, **11** [7–8] 871–919 (1990).

[12]W. Pannhorst, M. Spallek, R. Brückner, H. Hegeler, C. Reich, G. Grathwohl, B. Meier, and D. Spelmann, "Fiber-Reinforced Glasses and Glass Ceramics Fabricated by a Novel Process," *Ceram. Eng. Sci. Proc.*, **11** [7–8] 947–63 (1990).

[13]D. R. Dryell, and C. W. Freeman, "Trends in Design of Turbines for Aero Engines"; in Materials Development in Turbo-Machinery Design: *2nd Parsons International Conference*. Edited by D. M. R. Taplin, J. F. Knott, and M.H. Lewis. The Institute of Metals, Parsons Press, Trinity College, Dublin, Ireland, 1989.

[14]M. A. Karnitz, D. F. Graig, and S. L. Richlen, "Continuous Fiber Ceramic Composite Program," *Am. Ceram. Soc. Bull.* **70** [3] 430–35 (1991).

[15]S. R. Levine (Ed.), *Ceramics and Ceramic-Matrix Composites*, Vol. 3 in Flight Vehicle Materials, Structures and Dynamics—Assessment and Future Directions. American Society of Mechanical Engineers, New York, 1992.

[16]S. V. Nair and K. Jakus (Eds.), *Elevated Temperature Mechanical Behavior of Ceramic Matrix Composites*. Butterworth-Hienneman, Stoneham, MA, 1993.

[17]A. H. Chokshi and J. R. Porter, "Creep Deformation of Alumina Matrix Composites Reinforced with Silicon Carbide Whiskers," *J. Am. Ceram. Soc.*, **68** [6] C-144–C-145 (1985).

[18]J. R. Porter, F. F. Lange, and A. H. Chokshi, "Processing and Creep Performance of Silicon Carbide Whisker-Reinforced Silicon Nitride," *Mater. Res. Soc. Symp. Proc.*, **78,** 289–94 (1986).

[19]R. D. Nixon, S. Chevachaoenkul, M. L. Hukabee, S. T. Buljan, and R. F. Davis, "Deformation Behavior of SiC Whisker-Reinforced Si_3N_4," *Mater. Res. Soc. Symp. Proc.*, **78,** 295–302 (1987).

[20]D. A. Koester, R. D. Nixon, S. Chevacharoenkul, and R. F. Davis, "High Temperature Creep of SiC Whisker-Reinforced Ceramics"; pp. 139–45 in *Whisker- and Fiber-Toughened Ceramics*. Edited by R. A. Bradley, D. E. Clark, D. C. Larsen, and J. O. Stiegler. ASM International, Metals Park, OH, 1988.

[21]K. Xia and T. G. Langdon, "High Temperature Creep of Alumina Composites Containing SiC Whiskers," *Mater. Res. Soc. Symp. Proc.*, **120,** 265–70 (1988).

[22]P. Lipetzky, S. R. Nutt, and P. F. Becher, "Creep Behavior of an Al_2O_3–SiC Composite," *Mater. Res. Soc. Symp. Proc.*, **120,** 271–77 (1988).

[23]J. G. Baldoni and S. T. Buljan, "Creep and Crack Growth Resistance of Silicon Nitride Composites"; pp. 786–95 in *Ceramic Materials and Components for Engines*. Edited by V. J. Tennery. American Ceramic Society, Columbus, OH, 1989.

[24]B. J. Hockey, S. M. Wiederhorn, W. Liu, J. G. Baldoni, and S. T. Buljan, "Tensile Creep of SiC Whisker Reinforced Silicon Nitride"; presented at the Twenty-Seventh Automotive Technology Development Contractors Coordination Meeting, October 23–26, 1989.

[25]S. M. Wiederhorn and B. J. Hockey, "High Temperature Degradation of Structural Composites"; presented at the Seventh World Ceramics Congress, Montecatini Terme, Italy, June 24–30, 1990.

[26]P. Lipetzky, S. R. Nutt, D. A. Koester, and R. F. Davis, "Atmospheric Effects on Compressive Creep of SiC-Whisker-Reinforced Al_2O_3," *J. Am. Ceram. Soc.*, **74** [6] 1240–47 (1991).

[27]L. X. Han and S. Suresh, "High-Temperature Failure of an Alumina–Silicon Carbide Composite under Cyclic Loads: Mechanisms of Fatigue Crack-Tip Damage," *J. Am. Ceram. Soc.*, **72** [7] C-1233–C-1238 (1989).

[28]K. M. Prewo, "Fatigue and Stress Rupture of Silicon Carbide Fibre-Reinforced Glass-Ceramics," *J. Mater. Sci.*, **22,** 2695–701 (1987).

[29]F. Abbe, J. Vincens, and J. L. Chermant, "Creep Behavior and Microstructural Characterization of a Ceramic Matrix Composite," *J. Mater. Sci. Lett.*, **8,** 1026–1028 (1989).

[30]M. Khobaib and L. Zawada, "Tensile and Creep Behavior of a Silicon Carbide Fiber-Reinforced Aluminosilicate Composite," *Ceram. Eng. Sci. Proc.*, **12** [7–8] 1537–55 (1991).

[31]F. Abbe and J. L. Chermant, "Creep Resistance of SiC–SiC Composites under Vacuum"; pp. 439–48 in proceedings of the Fourth International Conference on Creep and Fracture of Engineering Materials and Structures. The Institute of Metals, London, U.K., 1990.

[32]J. W. Holmes, "Influence of Stress-Ratio on the Elevated Temperature Fatigue Life of a SiC Fiber-Reinforced Si_3N_4 Composite," *J. Am. Ceram. Soc.*, **74** [7] 1639–45 (1991).

[33]J. W. Holmes, "Tensile Creep Behavior of a Hot-Pressed SiC Fiber-Reinforced Si_3N_4 Composite," *J. Mater. Sci.*, **26,** 1808–14 (1991).

[34]Y. H. Park and J. W. Holmes, "Finite Element Modeling of Creep Deformation in Fiber-Reinforced Ceramic Composites," *J. Mater. Sci.*, **27,** 6341–51 (1992).

[35]J. W. Holmes, J. W. Jones, Y. Park, and C. Chui, "Tensile Creep Behavior of Fiber-Reinforced Ceramics"; pp. 72-1–72-14 in Proceedings of NASA HITEMP Review, Cleveland, OH, Oct. 1991. NASA Conference Publication No. 10082.

[36]X. Wu and J. W. Holmes, "Creep Recovery Behavior of Nicalon Calcium–Aluminosilicate Composites"; presented at the 17th Annual Conference on Composite Materials, January 1993.

[37]J. A. DiCarlo, "Creep of Chemically Vapour Deposited SiC Fibers," *J. Mater. Sci.*, **21,** 217–24 (1986).

[38]J. A. DiCarlo and G. N. Morscher, "Creep and Stress Relaxation Modeling of Polycrystalline Ceramic Fibers," NASA Technical Memorandum 105394, 1991.

[39]G. N. Morscher, J. A. DiCarlo, and T. Wagner, "Fiber Creep Evaluation by Stress Relaxation Measurements," *Ceram. Eng. Sci. Proc.*, **12** [7–8] 1032–1038 (1991).

[40]X. J. Ning and P. Pirouz, "The Microstructure of SCS-6 SiC Fiber," *J. Mater. Res.*, **6** [10] 2234–48 (1991).

[41]J. W. Holmes, "A Technique for Tensile Fatigue and Creep Testing of Fiber-Reinforced Ceramics," *J. Comp. Mater.*, **26** [6] 916–33 (1992).

[42]C. Cho, J. W. Holmes, and J. R. Barber, "Distribution of Matrix Cracks in a Uniaxial Composite," *J. Am. Ceram. Soc.*, **75** [2] 316–24 (1992).

[43]J. W. Holmes, and S. F. Shuler, "Influence of Loading Rate on the Monotonic Tensile Behavior of Fiber Reinforced Ceramics," Research Memorandum No. 102, September 1989. Ceramic Composites Research Laboratory, Department of Mechanical Engineering and Applied Mechanics, The University of Michigan, Ann Arbor, MI.

[44]J. W. Holmes, "Fatigue of Fiber-Reinforced Ceramics"; Ch. 12 in *Ceramics and Ceramic-Matrix Composites*, Vol. 3 in Flight Vehicle Materials, Structures and Dynamics—Assessment and Future Directions. Edited by S. R. Levine. American Society of Mechanical Engineers, New York, 1992.

[45]R. Kossowsky, D. G. Miller, and E. S. Diaz, "Tensile and Creep Strength of Hot-Pressed Si_3N_4," *J. Mater. Sci.*, **10,** 983 (1975).

[46]T. Fett, G. Himsolt, and D. Munz, "Cyclic Fatigue of Hot Pressed Si_3N_4 at High Temperatures," *Adv. Ceram. Mater.*, **1** [2] 179–84 (1986).

[47]M. K. Ferber and M. G. Jenkins, "Evaluation of the Strength and Creep-Fatigue Behavior of Hot Isostatically Pressed Silicon Nitride," *J. Am. Ceram. Soc.*, **75** [9] 2453–62 (1992).

[48]R. Y. Kim and A. P. Katz, "Mechanical Behavior of Unidirectional SiC/BMAS Ceramic Composites," *Ceram. Eng. Sci. Proc.*, **9,** 853–60 (1988).

[49]R. Y. Kim and Pagano, "Crack Initiation in Unidirectional Brittle-Matrix Composites," *J. Am. Ceram. Soc.*, **74** [5] 1082–90 (1991).

[50]J. W. Holmes and C. Cho, "Experimental Observations of Frictional Heating in a Fiber Reinforced Ceramic," *J. Am. Ceram. Soc.*, **75** [4] 929–38 (1992).

[51]D. S. Beyerle, S. M. Spearing, F. W. Zok, and A. G. Evans, "Damage and Failure in Unidirectional Ceramic-Matrix Composites," *J. Am. Ceram. Soc.*, **75** [10] 2719–25 (1992).

[52]R. T. Bhatt, "Matrix Density Effects on the Mechanical Properties of SiC Fiber-Reinforced Silicon Nitride Matrix Composites," *Ceram. Eng. Sci. Proc.*, **11** [7–8] 974–94 (1990).

[53]J.-F. LeCostaouec, Textron Specialty Materials, Lowell, MA; personal communication, June 1991.

[54]G. Simon and A. R. Bunsell, "Creep Behavior and Structural Characterization at High Temperatures of Nicalon SiC Fibers," *J. Mater. Sci.*, **19,** 3658–70 (1984).

[55]R. M. Arons and J. K. Tien, "Creep and Strain Recovery in Hot-Pressed Silicon Nitride," *J. Mater. Sci.*, **15,** 2046–58 (1980).

[56]S. Haig, W. R. Cannon, P. J. Whalen, and R. G. Rateick, "Microstructural Effects on the Tensile Creep of Silicon Nitride"; in *Creep: Characterization, Damage and Life Prediction*. Edited by D. A. Woodford, C. H. A. Townley, and M. Ohnami. ASM International, Metals Park, OH, 1992.

[57]F. F. Lange, D. R. Clarke, and B. I. Davis, "Compressive Creep of Si_3N_4/MgO Alloys, Part 2," *J. Mater. Sci.*, **15,** 611–15 (1980).

[58]G. E. Hilmas, J. W. Holmes, and R. Bhatt, "Tensile Creep of SiC-Fiber RBSN-Matrix Composites," to be submitted to *J. Am. Ceram. Soc.* □